4. Résultats et discussions

Les résultats de cette étude seront soumis dans un journal scientifique et se trouvent dans le manuscrit qui suit.

Synthèse des nanocatalyseurs hautement sélective pour la réduction du NO avec C_3H_6: Ag/Al_2O_3, Cu/Al_2O_3 et $Ag\text{-}Cu/Al_2O_3$

Robenson Cherizol, Driss Mrabet, Serge Kaliaguine, Trong-On Do
Department of Chemical Engineering, Laval University, Ste Foy (QC), Canada G1K7P4

Résumé

La réduction catalytique sélective (SCR) du NO est la stratégie la plus importante pour éliminer les émissions de NO_x provenant des moteurs à combustion interne. La réaction du NO avec le C_3H_6 a été étudiée dans plusieurs conditions, y compris en présence de hautes concentrations d'oxygène. Ag/Al_2O_3 a été retenu comme un catalyseur prometteur pour la réduction catalytique sélective des NO_x en N_2 par les hydrocarbures (HC-SCR) à l'échelle des essais de laboratoire comme dans le fonctionnement des moteurs diesel. Les étapes de l'élaboration d'un catalyseur d'argent actif pour des applications pratiques impliquent la connaissance du mécanisme, le choix correct de la teneur du métal et du support, d'ajustement de la concentration de l'hydrocarbure à être utilisé comme agent réducteur, etc.

Dans ce travail nous avons investigué et comparé des catalyseurs Ag/Al_2O_3 préparés par trois méthodes différentes (Ag/Al_2O_3(I), Ag/Al_2O_3(II) et Ag/Al_2O_3(C)) et finalement nous avons synthétisé Cu/Al_2O_3(I) et $Ag\text{-}Cu/Al_2O_3$(I) par la méthode en une seule étape. Tous les catalyseurs préparés ont contenu 3% Ag et10% Cu. La vitesse spatiale était de $19000h^{-1}$ pour les mêmes conditions catalytiques: 3000 ppm C_3H_6 +1000 ppm NO + (1; 5; 10 et 15) % O_2. On a constaté que la méthode de préparation du catalyseur ainsi que la concentration de l'oxygène exercent une influence importante sur l'activité catalytique. Le catalyseur Ag/Al_2O_3(I) préparé par la méthode en une étape a présenté la meilleure performance catalytique.

Synthesis of highly selective nanocatalysts for the reduction of NO with C_3H_6: Ag/Al_2O_3, Cu/Al_2O_3 and $Ag\text{-}Cu/Al_2O_3$

Robenson Cherizol, Driss Mrabet, Serge Kaliaguine, Trong-On Do
Department of Chemical Engineering, Laval University, Ste Foy (QC), Canada G1K7P4

Abstract

Selective catalytic reduction (SCR) of NO_x is the most important strategy to remove the NO_x emissions from internal combustion engines [1-2]. The reaction of NO with C_3H_6 has been studied in various conditions including high concentrations of oxygen. Ag/alumina has been found to be a promising catalyst for the selective catalytic reduction of NO_x to N_2 by hydrocarbons (HC-SCR) in laboratory tests as well as in full-scale diesel engine operation [3-4]. The steps in developing an active silver catalyst for practical applications involve knowledge of the mechanism, choice of the right metal content and correct support, adjustment of the concentration of the hydrocarbon to be used as a reducing agent, etc.

In this work, we investigated and compared Ag/Al_2O_3 catalysts prepared by three different methods (Ag/Al_2O_3(I); Ag/Al_2O_3(II) and Ag/Al_2O_3(C)) and finally we synthesized Cu/Al_2O_3(I) and $Ag\text{-}Cu/Al_2O_3$(I) by a one step method. All silver catalysts prepared contained 3% Ag and those containing copper had 10% Cu. The spatial velocity of 19000/h was implemented in the same catalytic conditions: 3000 ppm C_3H_6 +1000 ppm NO + (1; 5; 10 and 15) % O_2. It was found that the catalyst preparation method as well as the concentration of oxygen exerts a significant influence on catalyst activity. Catalyst Ag/Al_2O_3 (I) prepared by a one step method presented the best catalytic performance.

1- Introduction

The control of NO_x emission from automobiles remains challenging for both the industry and academic researchers. The selective catalytic reduction (SCR) of NO by hydrocarbons, in particular propene is currently believed to be a possible way to solve this problem and has therefore been extensively studied [5-9]. A large number of catalytic systems has been investigated including metal-zeolites, perovskites, supported metal and oxide/mixed oxide catalysts. For example, Cu-ZSM-5 was an effective catalyst for the SCR of NO, however, the zeolite based catalysts suffer from low hydrothermal stability and easy deactivation by carbonaceous and SO_2 poisoning [10]. Among them, silver based catalysts were deemed as the most effective materials for SCR of NO in excess oxygen in the presence of C_3H_6 or C_2H_5OH [10], and were intensively investigated, even in the presence of water vapour and SO_2 [11]. Seker et al. [12] compared Ag-Al_2O_3 catalysts prepared by different techniques, namely, co-precipitation, impregnation and single-step sol–gel methods for the SCR of NO_x by C_3H_6 and found that sol–gel-prepared catalysts had superior activity compared to other samples. The improved catalytic performance of sol–gel-prepared Ag/Al_2O_3 was attributed to a better dispersion of metal cations on the Al_2O_3 support. Highly isolated Ag cations, strongly bonded to alumina, are the active sites for the NO-SCR process [12-14].

On the other hand, alumina-supported copper (Cu/Al_2O_3) catalysts have recently become another focus as a metal oxide catalyst for the SCR of NO due to their low cost and catalytic performance. Shimizu et al. [15] found that Cu/Al_2O_3 with a high Cu content showed higher activity at low temperature and higher hydrothermal stability than Cu-ZSM-5 [16-17]. Recently, Kim et al. [18] reported that a 10 wt.% Cu/Al_2O_3 catalyst with a $CuAl_2O_4$ phase exhibited a high reactivity for the SCR of NO by C_3H_6. It seems that Cu-Al_2O_3 is a promising catalyst for NO removal [13]. Both Ag/Al_2O_3 and Cu/Al_2O_3 catalysts exhibit a high catalytic activity for the SCR of NO by C_3H_6; however, Ag/Al_2O_3 shows a higher catalytic activity as compared to Cu/Al_2O_3 [14]. It is believed that highly isolated metal cations (e.g., Ag and Cu) strongly bonded to alumina, are the active sites for the NO-SCR process [12-21].

Furthermore, we recently reported that using alumina as support for silver, the Ag/Al_2O_3 catalysts for the SCR of NO by C_3H_6 depend greatly on the alumina source used, such as AlOOH, Al_2O_3 and $Al(OH)_3$ for preparation [22]. However, a breakthrough has not yet been achieved proving the significance of metal-containing catalysts for commercial exhaust gas cleaning of Otto engines or diesel engines under road conditions. Specifically, the performance under lean conditions at lower temperatures required for exhaust gas cleaning of diesel-fuelled engines is not satisfactory.

Nanoscale materials have recently attracted great interest because of their size dependent characteristics and novel properties that cannot be achieved using their bulk counterparts [23]. This type of catalyst exhibits high catalytic activity toward different types of reactions, such as the NOx reduction and the CO oxidation at low temperatures [22-28]. Corma et al. [28] reported that nanocrystalline CeO_2-supported Au catalysts are two orders of magnitude more active than conventional Au/ CeO_2 catalysts for the CO oxidation. This might be due to altering electronic properties and a synergistic interaction between Au nano-clusters and nanosupport at the interface, such that the support does not act as an inert carrier but intervenes in the catalytic reactions [28-29]. Furthermore, the effectiveness of this type of catalysts for NO_x reduction depends strongly on the dispersion and the local structure of metal additives, which in turn depend on the loading and catalyst preparation technique.

In this study, we have developed a new route for the one step synthesis of Cu/Al_2O_3, Ag/Al_2O_3 and $Ag\text{-}Cu/Al_2O_3$ nanocomposite catalysts in the presence of oleylamine as a capping agent with high specific surface area for the purpose of obtaining best performing SCR catalysts. The obtained nanocomposite catalysts were characterized by XRD, TEM and TPR. Selective catalytic reduction (SCR) of NO with C_3H_6 over these catalysts was investigated and compared to those of the Ag/Al_2O_3(II) nanocomposite prepared by our two step method [29] and a conventional Ag/Al_2O_3(C) prepared by impregnation using commercial □-alumina powders as support. The influence of oxygen concentration in the feed gas mixture on the catalytic performances of these catalysts was also studied.

2- Experimental section

2.1. Preparation of catalysts

One step synthesis: Typically, for the synthesis of metal-Al_2O_3 nanocomposite catalysts, denoted as Ag/Al_2O_3(I), Cu/Al_2O_3(I), $Cu\text{-}Ag/Al_2O_3$(I), 0.02 g (0.01 mmol) of silver nitrate and/or 0.131 g (0.65 mmol) of copper acetate was added to 50 ml of toluene containing 1.4 g (5.2 mmol) of oleylamine. After complete dissolution, to the mixture, 0.75 g (3.7 mmol) aluminium isopropoxide was added. The mixture was stirred vigorously for 1 h at room temperature, then sealed in a Teflon-lined stainless-steel autoclave of 80 mL capacity and maintained at 180 °C for 20 h. The autoclave was then cooled down to room temperature. The nanocomposite products were precipitated with an excess ethanol and further isolated by centrifugation. The resulting solid products were dried at 105 °C and calcined at 550 °C for 4 h under air flow.

Two step synthesis: The synthesis of metal/metal oxide nanocomposite catalyst, namely, Ag/Al_2O_3(II) through the cooperative assembly of pre-synthesized oleylamine (OL)-capped Ag nanoparticles and OL-capped Al_2O_3 nanoparticles in toluene, was followed by the method described in ref. 29, and consists of two steps: (i) Synthesis of OL-capped Ag nanoparticles and OL-capped Al_2O_3 nanoparticles in toluene media. The pre-synthesized hydrophobic NPs of both metal and metal oxide were separately dispersed in toluene. (ii) The Ag NPs suspension and the Al_2O_3 NPs suspension with desired proportions were mixed, and clear/transparent suspension were obtained. These mixtures were submitted to evaporation. The dispersion of Ag and Al_2O_3 NPs was then locked in place by drying and then calcination at 550°C for 4 h.

For comparison, the conventional Ag/Al_2O_3sample, denoted as Ag/Al_2O_3(C) was also prepared by impregnation using commercial $\gamma\text{-}Al_2O_3$ powders as support (Alfa products, SA: 100 m^2/g) with a desired amount of silver nitrate aqueous solution, at room temperature for 6 h, then dried at 100 °C overnight, calcined under air flow at 550°C for 4 h.

2.2. Characterisation of materials

BET surface area, pore volume and pore diameter: BET surface areas of the Al_2O_3 based nanocomposite catalysts were obtained from N_2 adsorption/desorption isotherms measured at -196°C using an automated gas sorption system (NOVA 2000, Quantachrome) operating in continuous mode. The specific surface area was determined from the linear part of the BET curve (P/P_0 = 0.01-0.15). Pore volume and average diameter were obtained from pore size distribution curve, which was calculated from the desorption branch of N_2 adsorption/desorption isotherms using the Barret-Joyner-Halenda (BJH) formula.

Transmission Electron Microscopy (TEM): Particle size and morphology of the mateials were studied using transmission electron microscopy (TEM). TEM images were obtained on a JEOL JEM 1230 Transmission Electron Microscope operating at 120 kV. The nanocomposite materials were dispersed in toluene and cast onto a 200 mesh carbon-coated copper grid sample followed by evaporation at room temperature.

X-ray Powder Diffraction (XRD): XRD patterns were recorded using a Siemens D 5000 X-ray diffractometer using filtered CuKα (λ = 1.54062 Å) radiation (40 kV, 30 mA). The data were collected over a range of 20°– 80° 2θ with a scan step of 0.02° and an acquisition time of 1.2 s per step. Crystal domain sizes (D) were evaluated by means of the Scherrer equation after Warren's correction for instrumental broadening. The identification of the crystal phases took place using the JCPDS.

Temperature-Programmed Reduction (TPR): Prior to H_2-TPR, the sample (50 mg) was pretreated under a 10% O_2/He flow at 20 cm^3/min total flow rate (STP) for 1 h at 550°C; cooled down to room temperature under the same atmosphere; purged with 20 cm^3/min total flow at 5% H_2/Ar, and streamed with a rising temperature of up to 900°C at a constant heating rate of 5°C/min. The water in the effluent gas of the TPR process was condensed via a cold trap with a mixture of dry-ice and ethanol. H_2 consumption was monitored continuously by TCD using a flow of 20 cm^3/min of 5% H_2/Ar as a reference gas. The gas responses obtained by MS and TCD during transient studies were calibrated using standard mixtures.

2.3. Catalytic activity

Catalytic tests were performed under steady-state conditions in a quartz tube fixed-bed reactor. The system was heated externally via a tubular furnace, regulated by a temperature controller (Omega CN3240) via a thermocouple in contact with the catalyst bed, to raise the reactor temperature by step of 50°C/min from 150 °C to 600 °C. A feed gas with 1000 ppm NO, 3000 ppm C_3H_6 and (1, 5, 10 and 15)% oxygen with helium as a balance was fed to 50 mg of catalyst at a total flow rate of 60 ml/min, which corresponded to a $19000h^{-1}$ space velocity. N_2 and O_2 in the reactor effluent were analyzed with a HP 5890A gas chromatograph equipped with a molecular sieve column combined with a silicone column using a TCD detector. The effluent gases (C_3H_6, CO_2, H_2O, NO_2, CO) were monitored using an Infrared analyzer (FT-IR) model (FTLA 2000, ABB). The yields of NO and NO_2 were determined using a chemi-luminescence $NO/NO_2/NO_x$ analyzer (model 200AH, Advanced Pollution Instrumentation (API), USA).

3. Results and Discussion

3.1. Characterization

Table 1 summarizes the Cu and Ag loadings, BET surface area, pore volume and average pore diameters of the alumina-based nanocomposite samples obtained by the above discussed different methods. The Ag and Cu loadings of alumina based metal samples determined by AAS (Atomic Absorption Spectroscopy) were close to values of 3 wt% Ag and 10 wt% Cu for all the samples. The crystal phase analysis performed by XRD exhibits the γ-Al_2O_3 phase (JCPDS 29-0063) for all the calcined sample prepared by one step method; Ag/Al_2O_3(I), Cu/Al_2O_3(I) and Ag-Cu/Al_2O_3(I), suggesting that the γ-alumina phase can be obtained, even after calcination at relatively low temperature, 550°C for 4 h. However, for the Ag/Al_2O_3(II) sample prepared by two step synthesis after hydrothermal treatment under the same conditions (550°C, 4 h in air flow), two phases of γ-Al_2O_3 and α-Al_2O_3, were observed. Furthermore, the XRD patterns of Ag/Al_2O_3(I), Ag/Al_2O_3(II) and Ag/Al_2O_3(C) shown in Figure 1 did not contain visible additional peaks characteristic of Ag_2O (JCPDS 41-1104) or Ag^0 (JCPDS 04-0783) with respect to their alumina support. An explanation for this observation is that the loaded silver was of very small size and well dispersed over the alumina substrate. Similar results were also observed for the Cu/Al_2O_3 (I) and Ag-Cu/Al_2O_3 (I), no diffraction lines of Cu and Ag were seen on these samples. For the samples prepared by one step method, for example, for the Ag/Al_2O_3(I) sample, the XRD pattern exhibits broad diffraction lines which are characteristic of nanocrystal size alumina. The average crystal size was also calculated as ~8 nm based on the XRD peak at $2\theta \approx 66.5°$ using the Scherrer equation.

Table 1. Physicochemical properties of the calcined alumina-based nanocomposite catalysts prepared by one step method (I), two step method (II), and conventional impregnation(C).

Catalyst	Cu loading (wt %)	Ag loading (wt %)	BET surface area (m^2/g)	Pore volume (cm^3/g)	Pore diameter (Å)
Ag/Al_2O_3 (I)	0	3	420	0.95	62
Cu/Al_2O_3 (I)	10	0	225	1.30	50
Ag-Cu/Al_2O_3 (I)	10	3	180	0.40	60
Ag/Al_2O_3 (II)	0	3	415	0.63	85
Ag/Al_2O_3 (C)	0	3	95	0.70	185

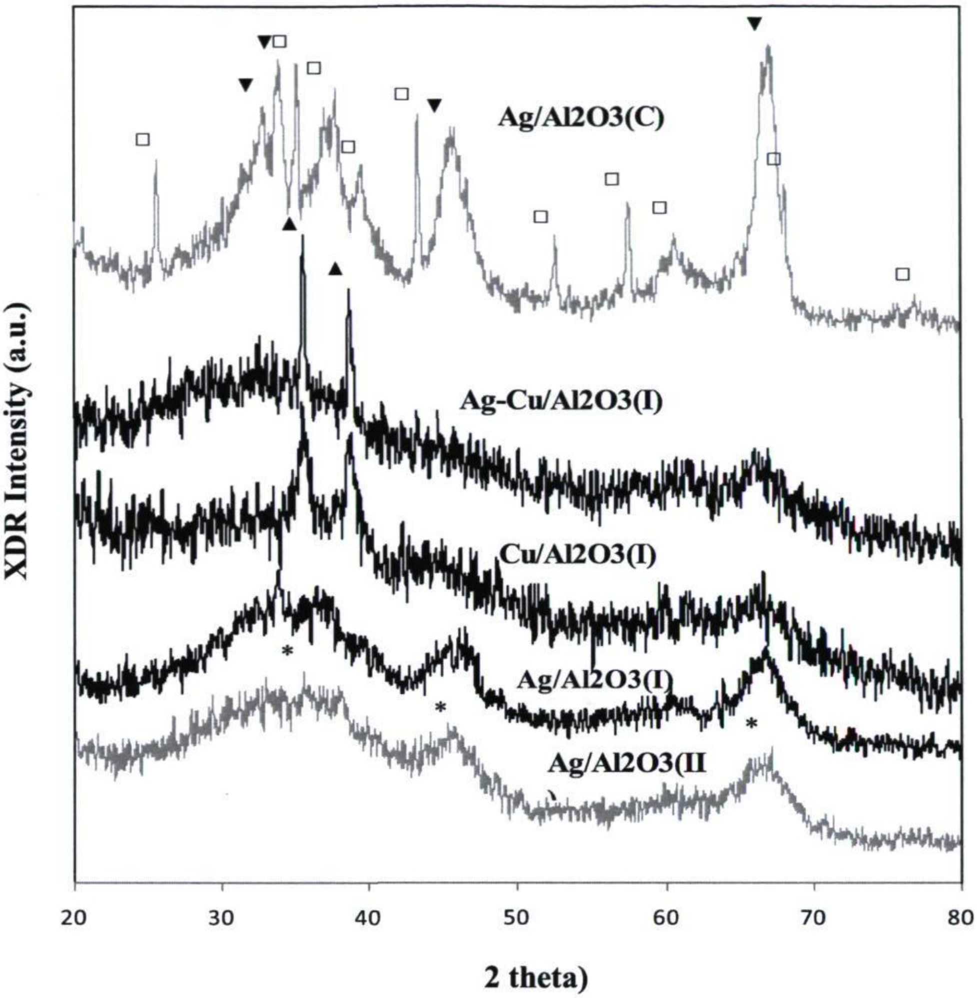

Figure 1. XRD spectra of the alumina-based silver nanocomposite and copper samples prepared by different methods after calcinations at 550°C for 4 h: Ag/Al_2O_3 (I), one step method, Ag/Al_2O_3 (II), two step method, Ag/Al_2O_3 (C), conventional impregnation method. (* γ-Al_2O_3, □ α-Al_2O_3), ▲CuO and ▼ δ-Al_2O_3

Figure 2 shows representative TEM pictures of the samples obtained by different methods; Ag/Al_2O_3 (I), Ag nanoparticles before assembly with Al_2O_3 nanoparticles for the preparation of Ag/Al_2O_3(I), Ag/Al_2O_3(II), and Ag/Al_2O_3(C). For the Ag/Al_2O_3(I) sample, no essential silver clusters were observed indicating very small clusters and high dispersion of silver on the alumina support. This observation is consistent with the XRD results. Oleylamine (OL)-capped Ag nanoparticles synthesized by a two-phase procedure according to the method of ref. 21 revealed almost regular spheres with diameters of 6-

8 nm. Regular Ag clusters without agglomeration were clearly found (Figure 2B). Representative TEM picture of the Ag/Al_2O_3(II) sample from self-assembled Ag-Al_2O_3 NPs is shown in Figure 2C revealing high dispersion of Ag clusters throughout large domains. The NPs retained however their individual size and shape. For Ag/Al_2O_3(C), small Ag clusters were observed. However, there seems to be less uniform Ag clusters and some aggregates were found (Fig. 2D).

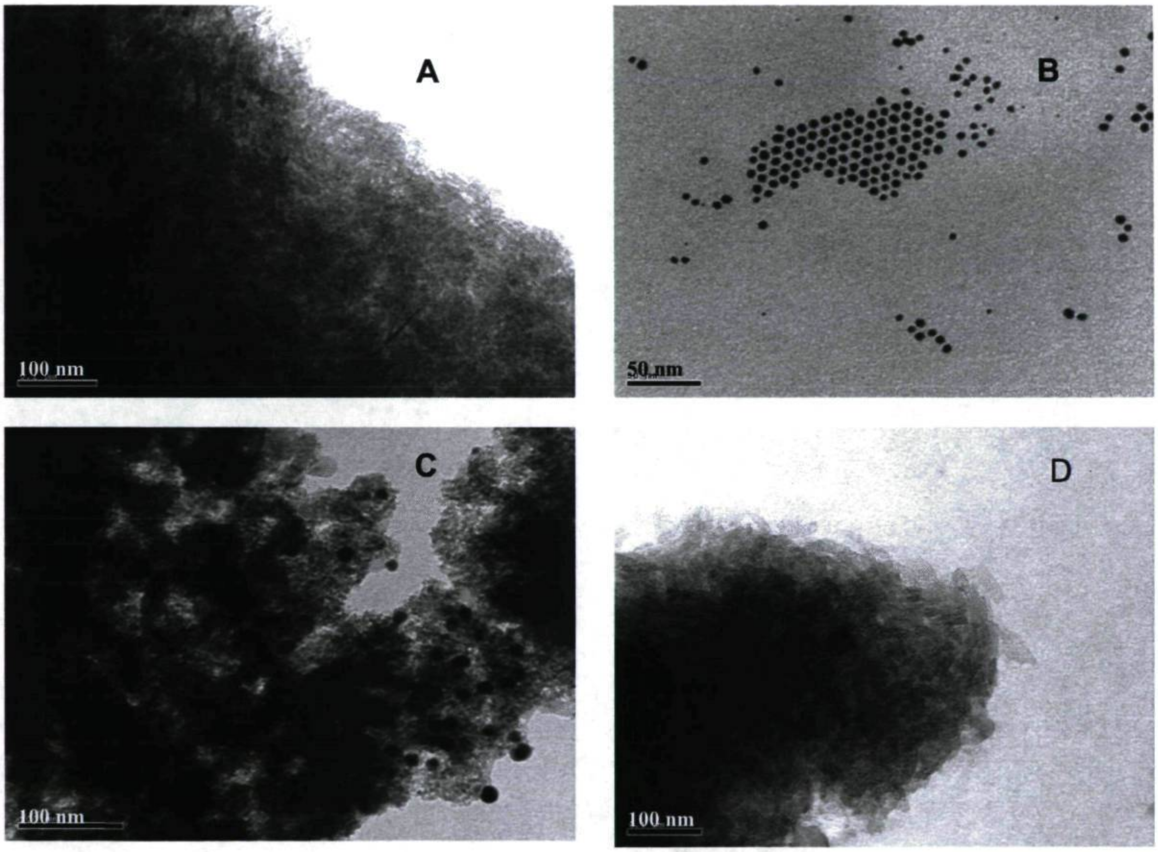

Figure 2. Representative TEM images of various catalyst samples prepared by different methods: (A) Ag/Al_2O_3 (I), one step method, (B) pre-synthesized Ag nanoparticles before cooperative assembly with Al_2O_3 nanoparticles, (C) Ag/Al_2O_3 (II), two step method, and (D) Ag/Al_2O_3 (C), conventional impregnation method.

BET specific surface area, pore volume and average pore diameter of the prepared samples were derived from nitrogen adsorption/desorption isotherms (Table 1). Nitrogen adsorption/desorption isotherms and the corresponding BJH desorption pore size distribution (Inset) of the Ag/Al_2O_3(I) and Cu/Al_2O_3(I) samples prepared by one step method are shown in Figure 3. A hysteresis loop at relatively high pressure ($P/P_0 > 0.4$) which is characteristic of mesopore structure was observed. High surface area (420 and 415 m^2/g) and average pore diameter (62 and 50 Å) were found for Ag/Al_2O_3(I) and Cu/Al_2O_3(I), respectively, suggesting that the samples prepared by our one step method have a relatively high surface to volume ratio. As shown in Table 1, the Cu-Ag/Al_2O_3(II) sample still retained a relatively high surface area (180 m^2/g). The decrease in surface area as compared to the Ag/Al_2O_3(I) and Cu/Al_2O_3(I) could be related to the simultaneous presence of Cu and Ag on the alumina support. Taking into account the XRD data which shows a transformation of the amorphous phase observed before calcination to γ-Al_2O_3 phase after calcination at quite low temperature (550°C) for the sample prepared by our one step method, the formation of the gamma alumina phase containing nanocrystal domains is deemed as the main reason for the enhancement in surface area. The Ag/Al_2O_3 (II) sample displayed also a high surface area of 225 m^2/g. This surface area value corresponds to the theoretical surface area calculated from the TEM average particle size. This indicates the nanoparticle surface is preserved after calcination [21]. The specific surface area of the sample prepared by conventional method using γ-Al_2O_3 decreased a little ($S = 95$ m^2/g) compared to the starting γ-Al_2O_3 ($S=100$ m^2/g).

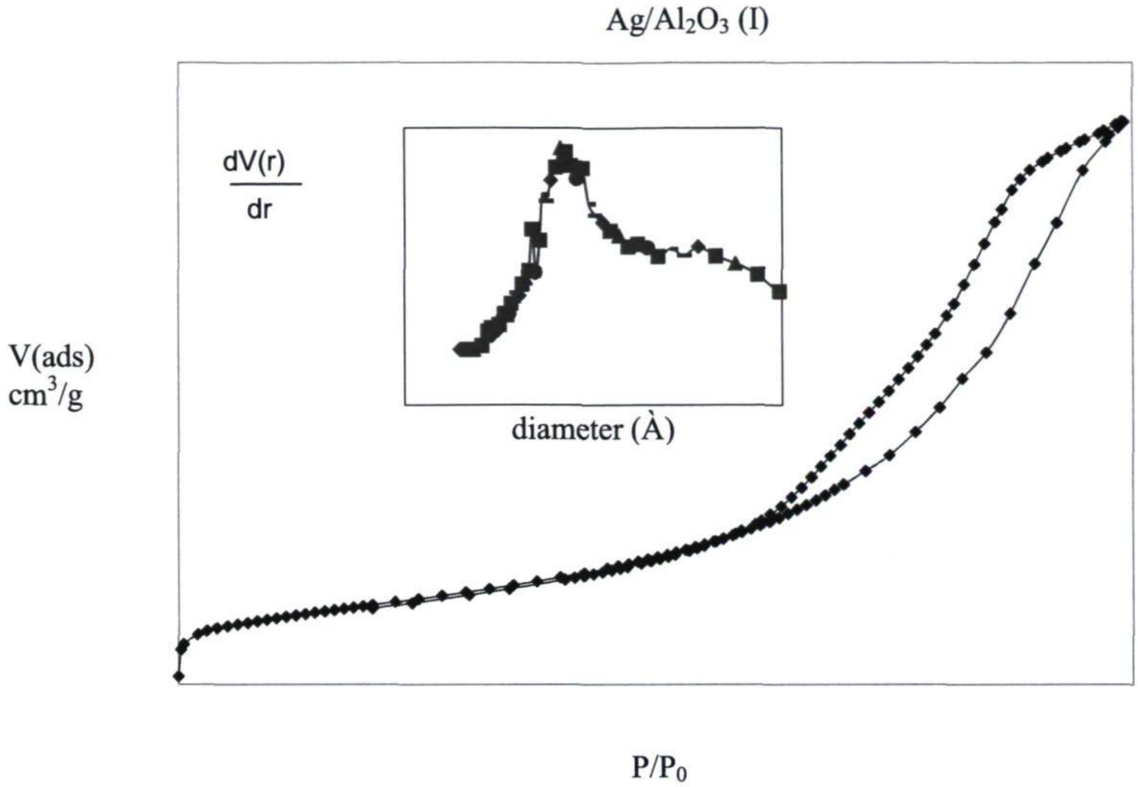
Ag/Al$_2$O$_3$ (I)
dV(r)/dr
diameter (À)
V(ads) cm^3/g
P/P$_0$

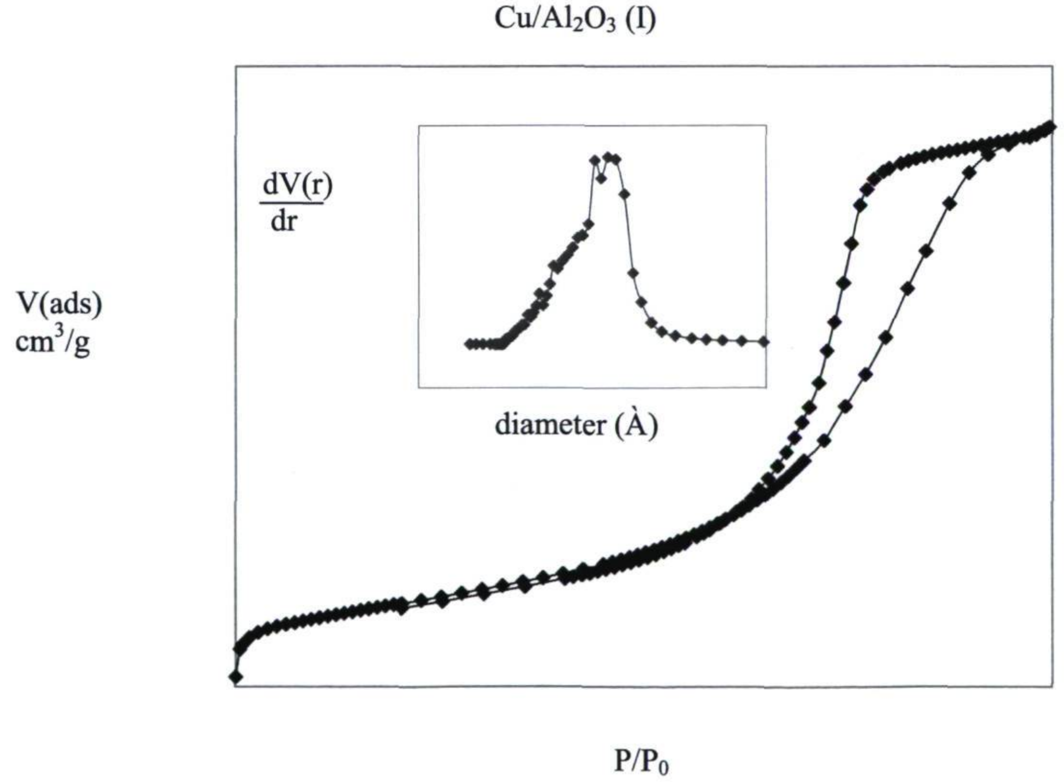
Cu/Al$_2$O$_3$ (I)
dV(r)/dr
diameter (À)
V(ads) cm^3/g
P/P$_0$

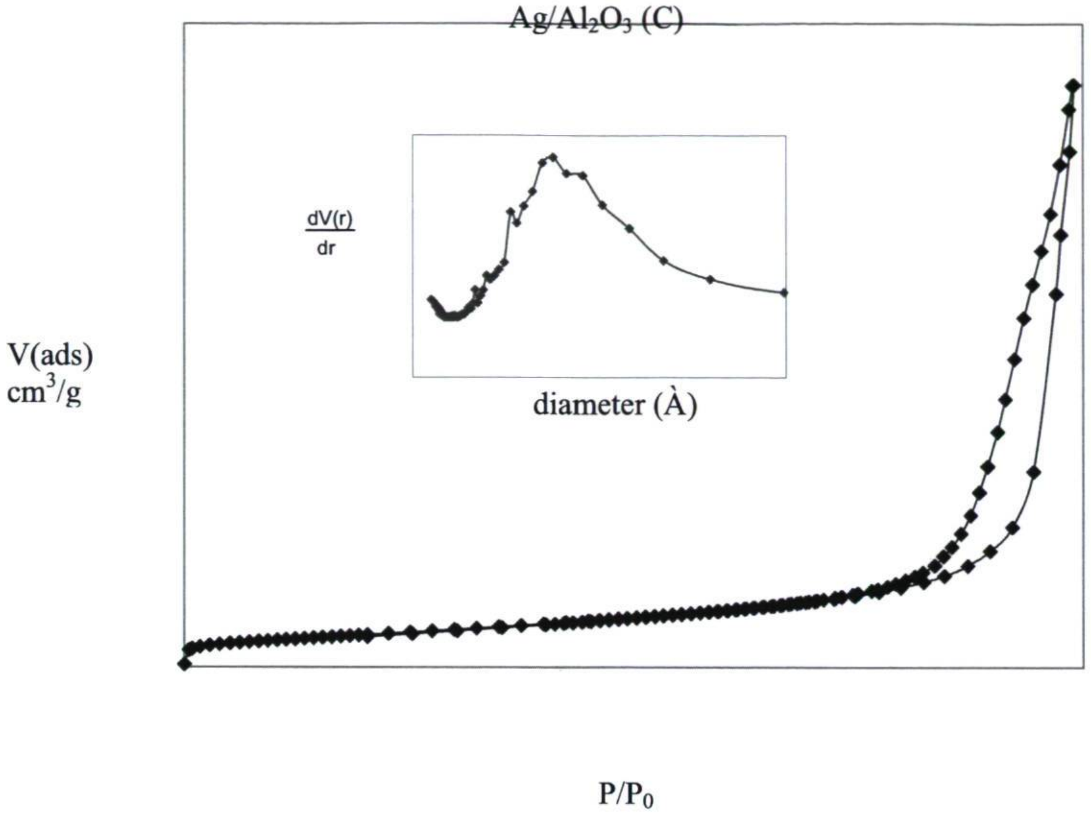

Ag/Al_2O_3 (C)
$\frac{dV(r)}{dr}$
diameter (À)
V(ads)
cm^3/g
P/P_0

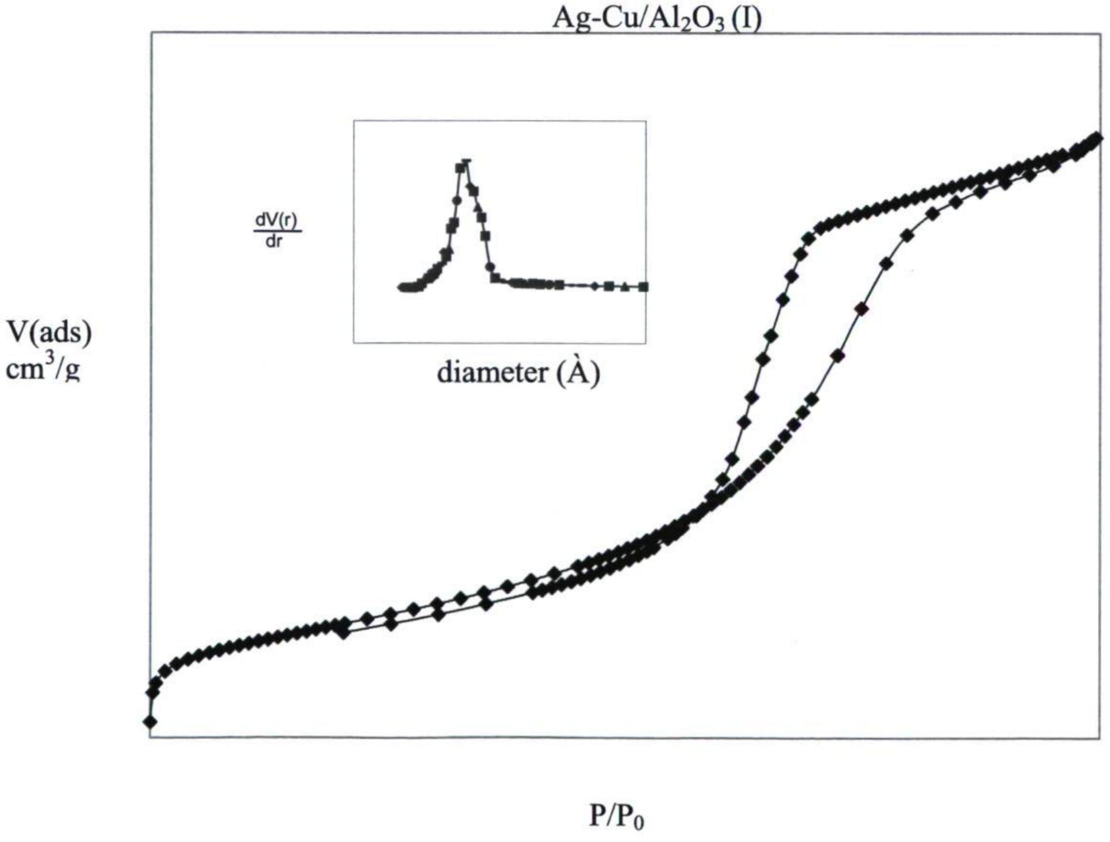

$Ag\text{-}Cu/Al_2O_3$ (I)
$\frac{dV(r)}{dr}$
diameter (À)
V(ads)
cm^3/g
P/P_0

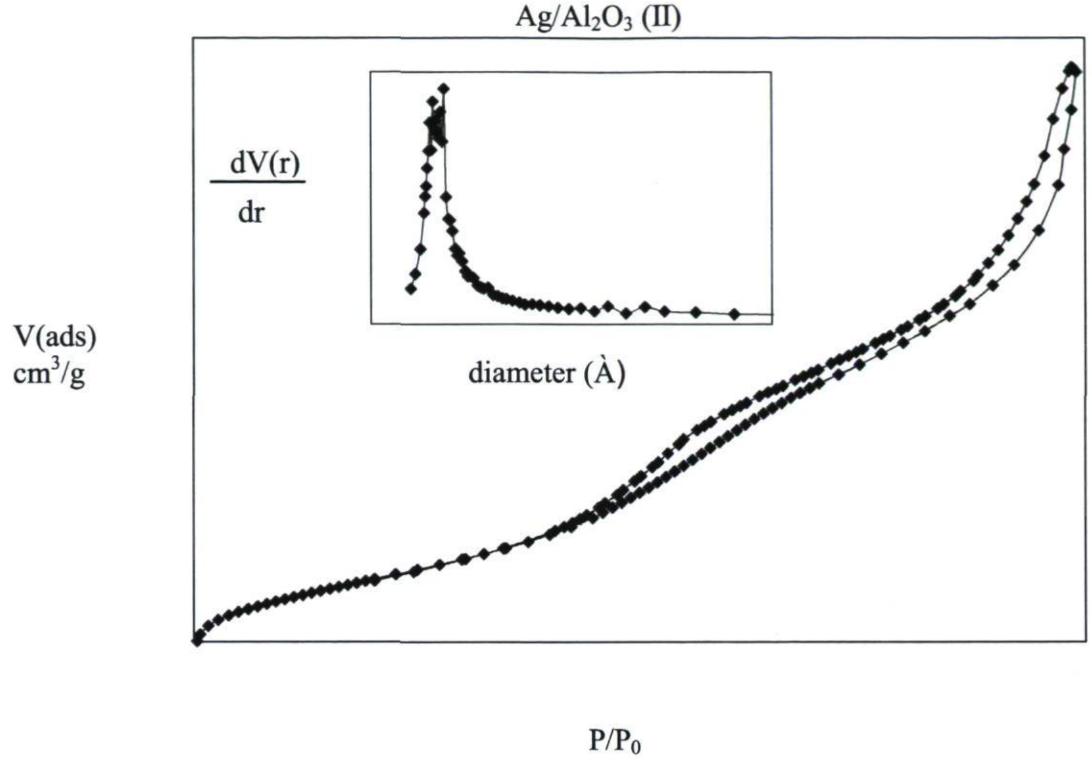

Figure 3: Nitrogen adsorption/desorption isotherms and pore diameter distribution (Inset) of the calcined samples prepared by different methods.

H_2-temperature-programmed reduction (H_2-TPR): The reducibility of the prepared samples was investigated by H_2-temperature-programmed reduction (H_2-TPR). The reduction profiles of the calcined Ag/Al_2O_3(I), Cu/Al_2O_3(I) and $Cu\text{-}Ag/Al_2O_3$(I) samples are shown in Figure 4. The Ag/Al_2O_3(I) sample shows overlapping reduction peaks at relatively high temperature (250 – 600 °C). A broad reduction peak at high temperature could be owing to the strong interaction of isolated silver oxide species with the alumina support and their high dispersion in the alumina matrix. Furthermore, a weak reduction peak could be due to a large fraction of silver already reduced in a metallic state after calcination because of its low thermal stability [23-24]. This is consistent with the previous observation that very small silver oxide clusters could not be detected by XRD. For the calcined Cu/Al_2O_3(I) sample, a sharp peak appeared at ~240 °C. This peak can be attributed to the reduction of isolated Cu^{2+} species to Cu^{+} and partial reduction of surface

$CuAl_2O_4$ to $CuAlO_2$ [13-15]. However, for the Ag-Cu/Al_2O_3 sample, the TRP profile is different from those of the corresponding monometallic samples. As seen in Figure 4, the bimetallic sample exhibits three broad reduction peaks at lower temperatures compared to those of the corresponding monometallic samples. The presence of metallic silver in the Ag-Cu/Al_2O_3 catalyst after calcination, could promote the reduction of CuO through hydrogen spillover. Hydrogen that dissociates on the surface of metallic Ag could migrate to the surface of CuO and support, resulting in Cu being reduced at much lower temperatures in the bimetallic catalysts.

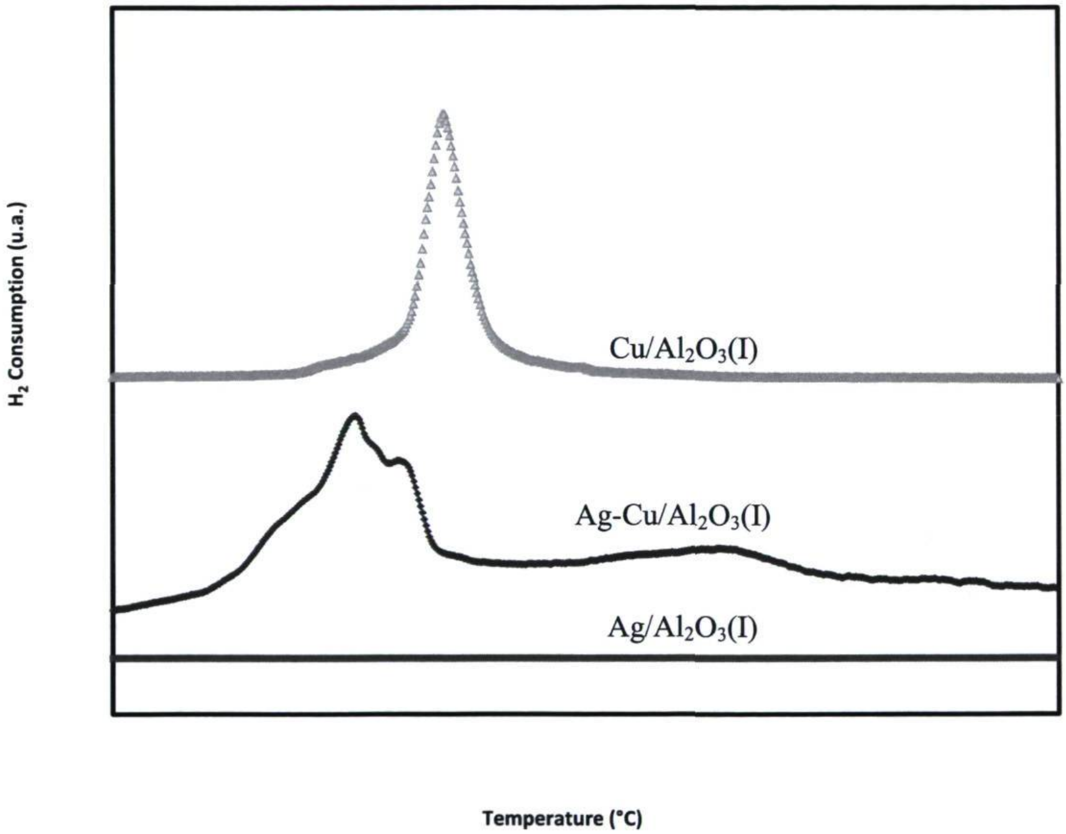

Fig. 4. H_2-TPR profiles of the calcined alumina-based samples: Ag/Al_2O_3, Cu/Al_2O_3 and Ag-Cu/Al_2O_3.

3.2. Catalytic activity

Fig. 5a shows the NO reduction conversion over the Ag/Al_2O_3 (I); Cu/Al_2O_3 (I) and $Ag-Cu/Al_2O_3$ (I) catalysts prepared by the same method (one step method). It can be seen that there are some similar trends in NO reduction behaviours with Ag and Cu content irrespective of the catalyst.

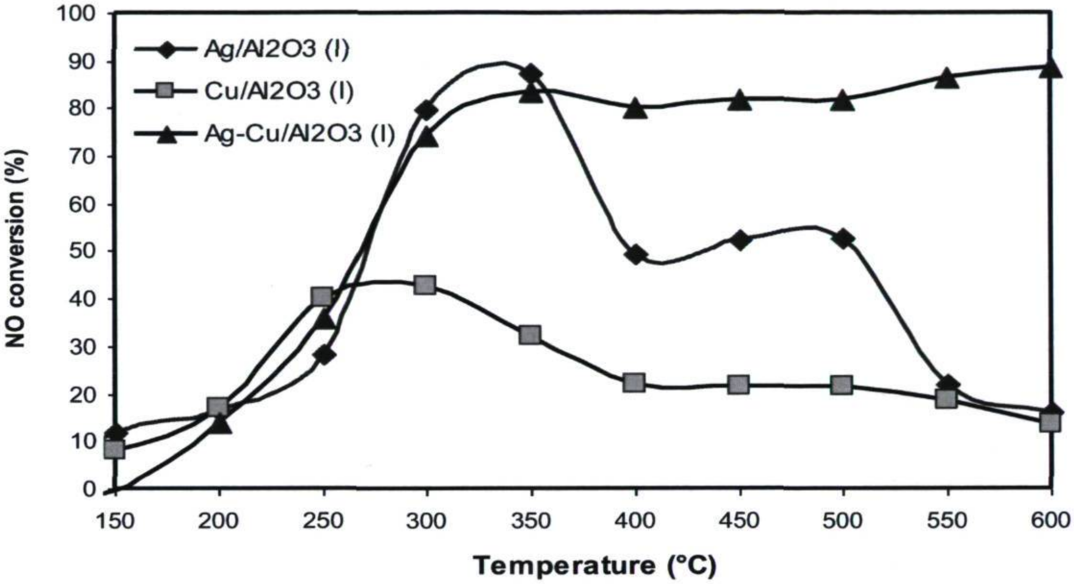

Fig. 5a: Catalytic performance of the alumina-based samples in C_3H_6-SCR of NO. Conditions: GHSV= $19000h^{-1}$, 1000 ppm NO, 3000 ppm C_3H_6, 10% O_2.

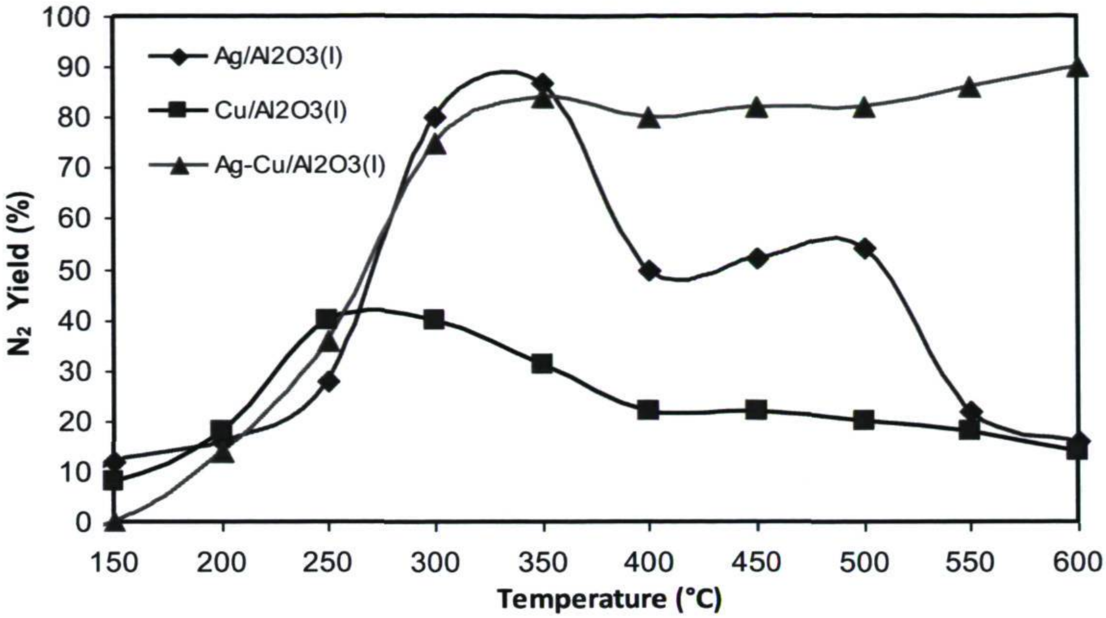

Fig. 5b. Catalytic performance of the alumina-based samples in C_3H_6-SCR of NO. Conditions: GHSV= $19000h^{-1}$, 1000 ppm NO, 3000 ppm C_3H_6, 10% O_2.

The NO conversion as a function of temperature at high O_2/NO reactant ratio over Ag/Al_2O_3(I), Cu/Al_2O_3(I) and Ag-Cu/Al_2O_3(I) is shown in Figure 5a. Increasing temperature increased the NO conversion, C_3H_6, O_2 conversion and N_2 yield (Fig. 5b) in the range of 200 – 350°C. Further increasing temperature above 350°C could decrease NO conversion and N_2 yield due the dominance of C_3H_6 oxidation at high temperature, except on Ag-Cu/Al_2O_3 (I) which shows no such decrease.

For the Ag/Al_2O_3(I) and Ag-Cu/Al_2O_3(I) the high activity of the catalysts is attributed to the surface area, the preparation method, the pore distribution and pore volume. The NO conversion passed through a maximum of 89% at 350°C for Ag/Al_2O_3(I) and then declined down to 50% at 400°C; 85% for Ag-Cu/Al_2O_3(I) at 350°C and kept stable until 600°C. With the addition of Cu, the catalytic activity has become stable due the good dispersion of Cu at the surface of Ag/Al_2O_3(I) and the good pore distribution. The low activity of the Cu/Al_2O_3 (I) can be attributed to the pore distribution and pore volume of this type of catalysts (Fig 5).

It is believed that this important lean-NOx activity arose in part from the high dispersion of Ag and Cu, where the catalysts are formed from nanoparticles, and the synergistic effects from the interface of both metal and metal oxides nanoparticles are the origin of the high catalytic activity. The synergism between these metal components could have allowed the activated propylene species, created on Cu when added to Ag/Al_2O_3(I) to improve the reduction of NO. Other particularity of this catalyst is the reduction occurred at low temperature, for instance from 250°C it was observed 50% conversion of NO to N_2, and also, the stability in the catalytic activity was completely improved when Cu was added at Ag/Al_2O_3(I). Thus, the nanocomposites approach resulted to excellent synergism between the active components that substantial increases in propylene conversions were achieved without significant reduction in selectivity for the latter three catalysts.

3.2.1. Reaction of NO reduction over Ag/Al_2O_3 prepared by different methods

Figure 6 shows NO conversion (6a) and N_2 yield (6b) obtained with the three catalysts Ag/Al_2O_3(I), Ag/Al_2O_3(II) and Ag/Al_2O_3(C). The standard test conditions are 1000 ppm NO; 3000 ppm C_3H_6; 10%O_2 and 19000h^{-1} of GHSV. The best performances for NO selective catalytic reduction to N_2 were obtained with Ag/Al_2O_3 (I) giving an NO conversion of 90% and N_2 yield of 89% at a temperature as low as 350°C. For the catalyst Ag/Al_2O_3 (II) a maximum NO conversion of 60% and N_2 yield of 56% were obtained and similar values were kept over a wide temperature range with a plateau from 300 to 450°C. The conventional catalyst Ag/Al_2O_3 (C) prepared with commercial alumina offered a maximum NO conversion of 44% and N_2 yield of 44% at the temperature of 350°C.

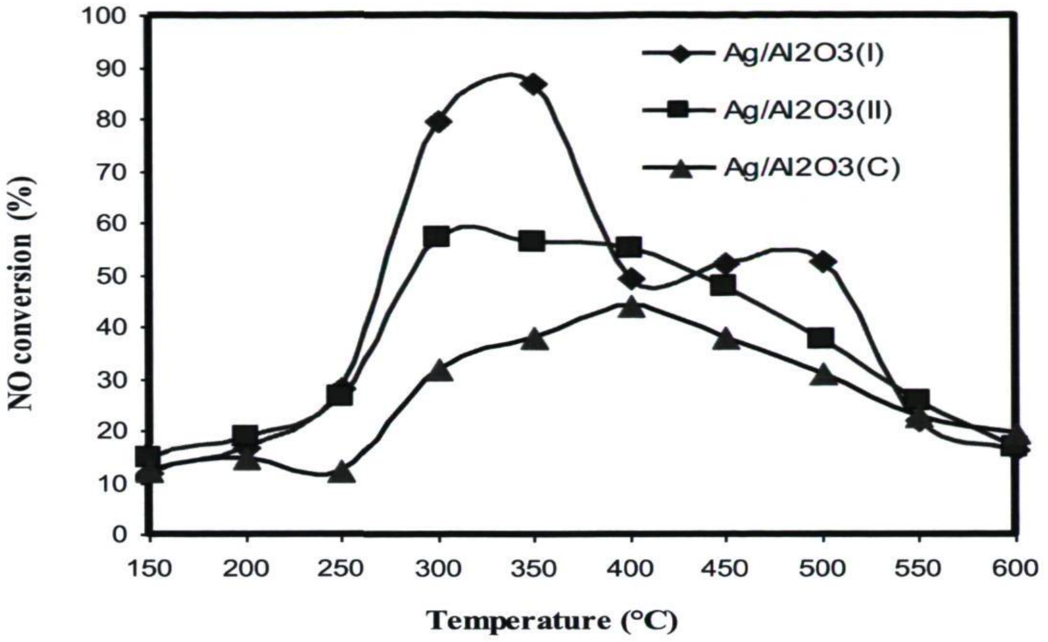

Fig. 6a. Catalytic performance of the alumina-based samples in C_3H_6-SCR of NO prepared by different methods. Conditions: GHSV= 19000h^{-1}, 1000 ppm NO, 3000 ppm C_3H_6, 10% O_2.

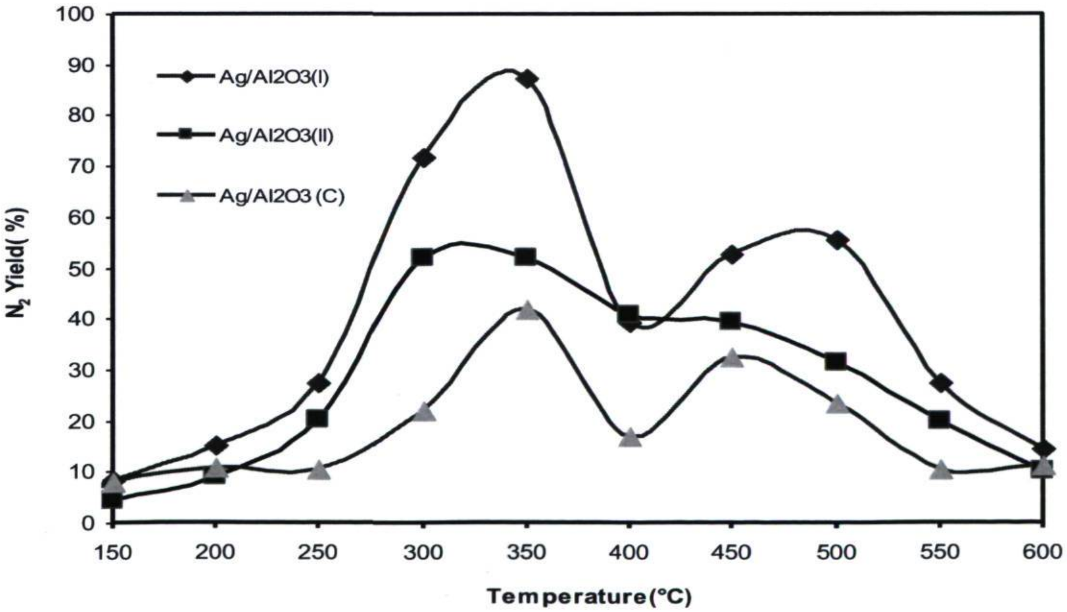

Fig. 6b. Catalytic performance of alumina-based samples in C_3H_6-SCR of NO prepared by different methods. Conditions: GHSV= 19000h^{-1}, 1000 ppm NO, 3000 ppm C_3H_6, 10% O_2.

The synthesis methods and the alumina source play a very important role in the catalytic activity as can be observed from Fig. 6a and 6b. The Ag/Al_2O_3(I) prepared in one step presents an excellent catalytic performance with high catalytic. The two step method used to synthesize Ag/Al_2O_3(II) is another very important way to prepare nanoparticles for the NO reduction since its presents thermally stable activity compared with others catalysts.

All tests were performed in the reaction conditions, with the same content of silver (3%), same surfactant and temperature of calcination. Table 2 presents a summary of the catalytic performances of the catalysts at 10% O_2 and same other catalytic conditions.

Table 2. Catalytic performance of different catalysts.
Conditions: GHSV= $19000h^{-1}$, 1000 ppm NO, 3000 ppm C_3H_6, 10% O_2

Catalyst	Temperature (°C)	NO Maximum Conversion (%)	N_2 Yield (%)	N_2 Selectivity (%)	C_3H_6 Conversion (%)
Ag/Al_2O_3 (I)	350	87	87	100	71
Ag/Al_2O_3 (C)	400	38	42	95	96
Ag/Al_2O_3 (II)	350	56	52	98	82
Cu/Al_2O_3 (I)	300	40	38	98	100
$Ag\text{-}Cu/Al_2O_3$ (I)	350	85	85	100	88

3.2.2. Effect of O_2 feed concentration

The best performing silver catalyst Ag/Al_2O_3(I) was further submitted to other catalytic tests at different concentrations of oxygen. Fig. 7 shows the catalytic performance of Ag/Al_2O_3(I) as a function of temperature for various oxygen contents keeping the same spatial velocity. Large differences in NO conversion were observed. However, with this catalyst, in this work, high conversions were found in the presence of oxygen. According Fig.7a the best reduction was found for a rather high concentration of oxygen between 5 and 10%.

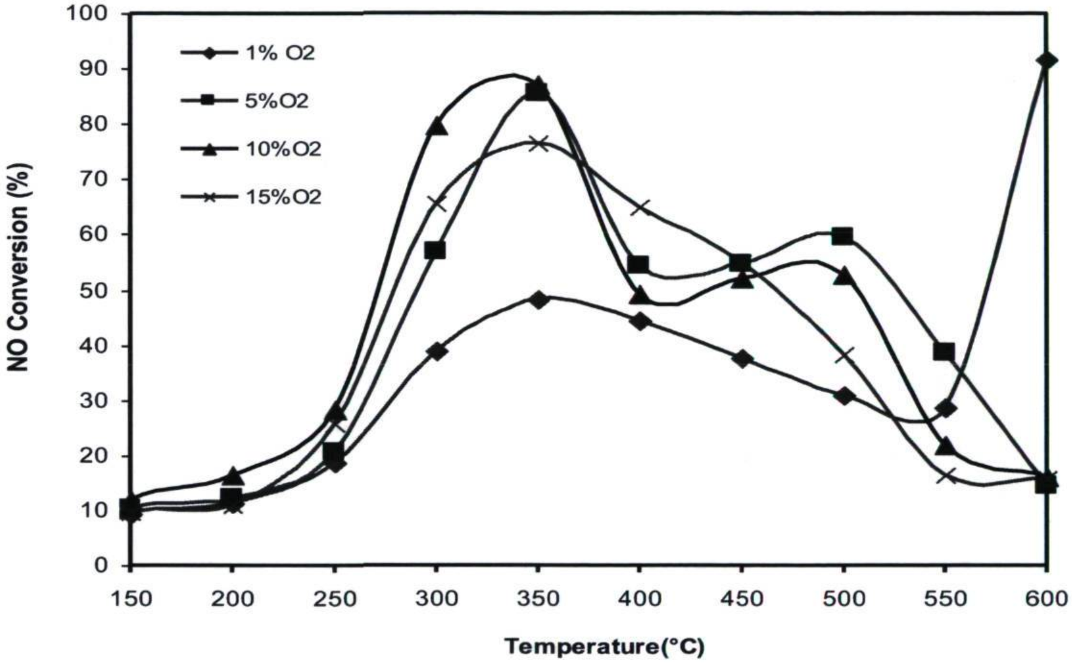

Fig. 7a. Effect of O_2 feed concentration on catalytic behaviour over Ag/Al_2O_3 (I). Conditions: GHSV= $19000h^{-1}$, 1000 ppm NO, 3000 ppm C_3H_6.

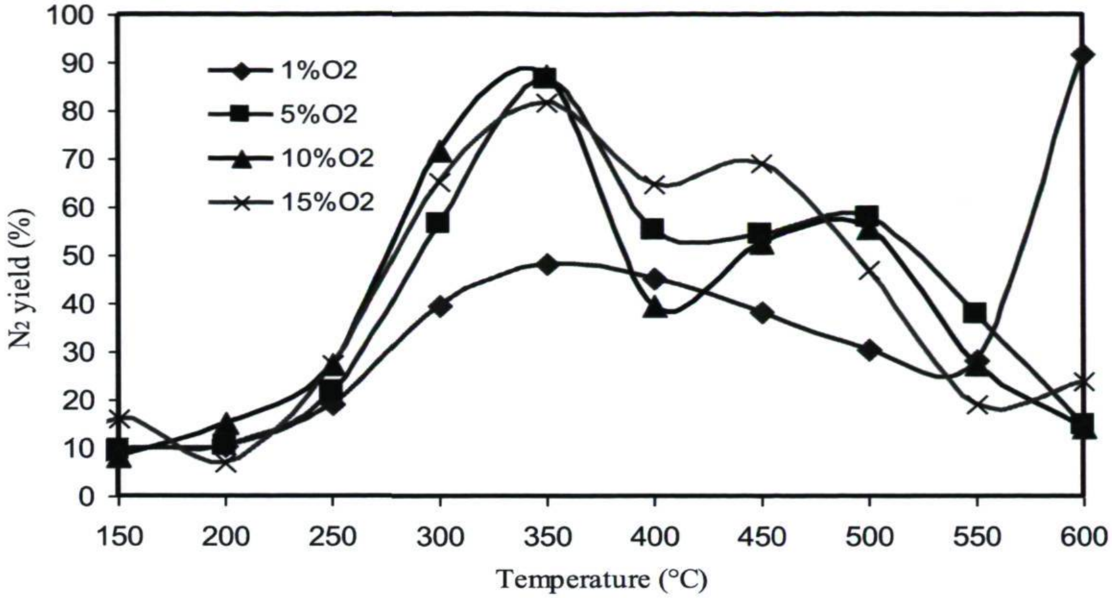

Fig. 7b. Effect of O_2 feed concentration on catalytic behaviour over Ag/Al_2O_3 (I). Conditions: GHSV= $19000h^{-1}$, 1000 ppm NO, 3000 ppm C_3H_6.

3. 2. 3. Comparison with other catalysts for 1% O_2

Compared to the corresponding values obtained in the presence of high concentrations of oxygen, both NO conversion and N_2 yield over Ag/Al_2O_3 (I) and Ag-Cu/Al_2O_3 (I) were noticeably lower (especially at low-temperatures) as the feed contained only 1% O_2 (Fig. 8). The best catalytic performances were obtained for Cu/Al_2O_3(I) in the presence of 1% oxygen (Fig. 8a and 8b).

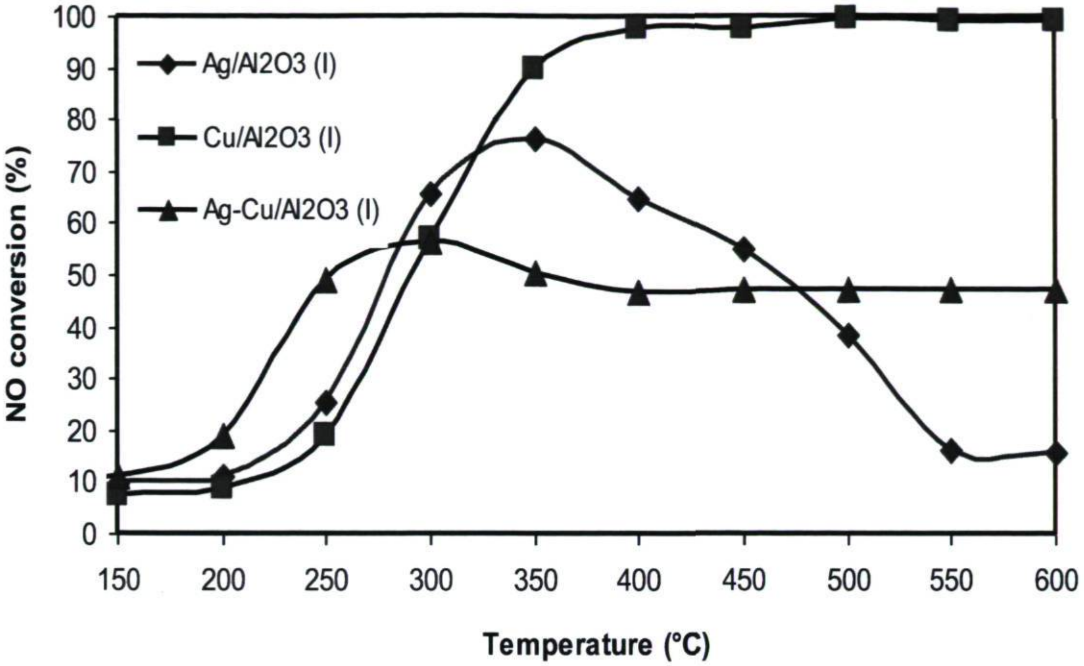

Fig. 8a. Catalytic performance of the alumina-based samples in C_3H_6-SCR of NO. Conditions: GHSV= $19000h^{-1}$, 1000 ppm NO, 3000 ppm C_3H_6, 1% O_2

Thus, the best N_2 yield (100%) was obtained with Cu/Al_2O_3 (I) at a temperature from 400°C to 600°C. When the Cu was added to Ag/Al_2O_3(I), this catalyst Ag-Cu/Al_2O_3(I) was able to convert only 55% of NO to N_2 at 300°C, but from 350°C the NO conversion declined down to 50% and was kept stable until 600°C.

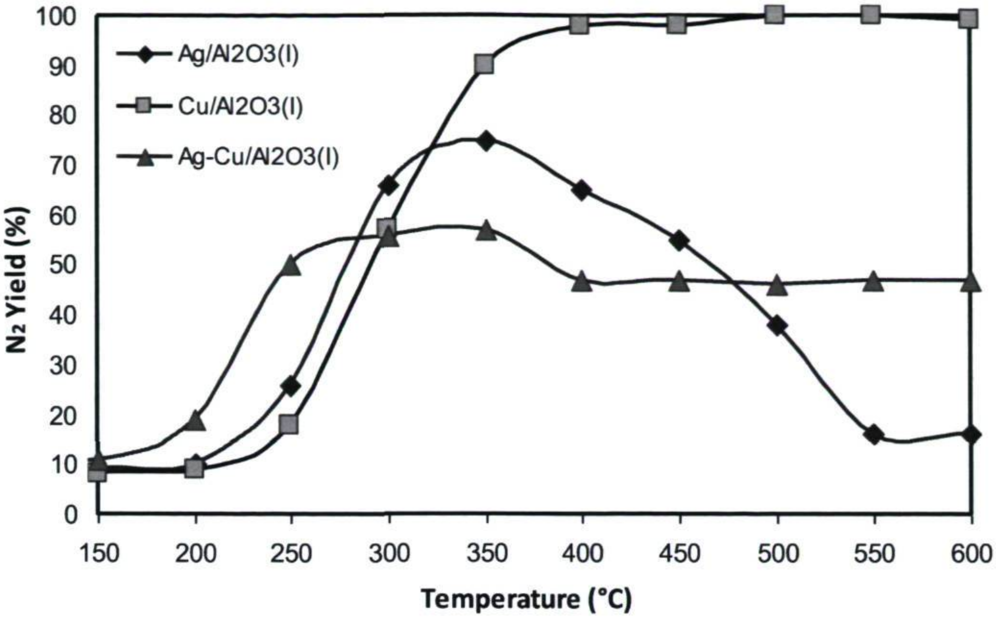

Fig. 8b. Catalytic performance of alumina-based samples in C_3H_6-SCR of NO. Conditions: GHSV= 19000h^{-1}, 1000 ppm NO, 3000 ppm C_3H_6, 1% O_2

4. Conclusion

The activity of the catalysts for NO reduction in the presence of C_3H_6 is largely dependent on the method of catalyst preparation and Ag or Cu content.

Nanoparticles alumina-supported catalysts active for the selective catalytic reduction SCR of NO by propylene were synthesized by new methods. In the first series for Ag/Al_2O_3(I), we obtained a high specific surface area ($420m^2/g$).

The interaction of metal particles with their oxide support can alter the electronic; the catalytic properties of the metal and can play a critical role in determining particle morphology and maintaining dispersion.

The Ag/Al_2O_3(II) catalyst prepared in two steps led to $415m^2/g$ specific area. These catalysts (Ag/Al_2O_3 (I) and Ag/Al_2O_3(II)) presented a very interesting catalytic activity in compared to the conventional catalyst Ag/Al_2O_3(C) with a specific area of $95m^2/g$.

But, the catalyst Ag/Al_2O_3(I) presents a thermal instability at a temperature superior to 400°C; for this reason we prepared, by the same preparation method, Cu/Al_2O_3(I) and $Ag\text{-}Cu/Al_2O_3$(I) so as to study the catalytic performances. In presence of high oxygen, the catalyst Cu/Al_2O_3(I) presented a low selective catalytic reduction. The bimetallic catalyst presented the best performance in the presence of different concentrations of oxygen and presented the thermal stability until 600°C. The significantly improved activity was attributed to synergism between better propylene activation and the high specific area.